MITSUBISHI ELECTRIC RESEARCH LABORATORIES
http://www.merl.com

Static voltage stability detection using local measurement for microgrids in a power distribution network

Wang, Z.; Sun, H.; Nikovski, D.N.

TR2015-147 December 2015

Abstract

Microgrid, integrated with generation, storage, and load, either produces or consumes power. When power consumption increases at a microgrid's point of common coupling (PCC), the entire power distribution network is at risk of voltage collapse. Critical load impedance and continuation power flow were currently used to assess static voltage stability in power systems. Critical load impedance was derived based on a Thevenin equivalent circuit model, but information used to derive the equivalent circuit is usually not available and accurate parameter estimation takes time. Because continuation power flow used approximation, this method is not accurate unless close to voltage collapse. To predict impending voltage collapse for a microgrid, this paper introduces a static voltage stability detector that only uses local measurements available at the microgrid's PCC. A voltage stability index depicts the distance of microgrid's power consumption from voltage collapse. Therefore, microgrid manager needs to take more urgent action when the index is smaller. Furthermore, microgrid manager predicts voltage stability index once a local load forecast is available. Compared with existing techniques, this voltage stability detector is accurate and easy to implement for microgrids in a power distribution network.

2015 IEEE Conference on Decision and Control (CDC)

Static voltage stability detection using local measurement for microgrids in a power distribution network

Zhao Wang[1], Hongbo Sun[2] and Daniel Nikovski[2]

Abstract— **Microgrid, integrated with generation, storage, and load, either produces or consumes power. When power consumption increases at a microgrid's point of common coupling (PCC), the entire power distribution network is at risk of voltage collapse. Critical load impedance and continuation power flow were currently used to assess static voltage stability in power systems. Critical load impedance was derived based on a *Thevenin* equivalent circuit model, but information used to derive the equivalent circuit is usually not available and accurate parameter estimation takes time. Because continuation power flow used approximation, this method is not accurate unless close to voltage collapse. To predict impending voltage collapse for a microgrid, this paper introduces a static voltage stability detector that only uses local measurements available at the microgrid's PCC. A voltage stability index depicts the distance of microgrid's power consumption from voltage collapse. Therefore, microgrid manager needs to take more urgent action when the index is smaller. Furthermore, microgrid manager predicts voltage stability index once a local load forecast is available. Compared with existing techniques, this voltage stability detector is accurate and easy to implement for microgrids in a power distribution network.**

I. INTRODUCTION

Microgrid concept is proposed to improve power quality and reliability by providing local power service [1], primarily in power distribution networks. Specifically, microgrids incorporate distributed energy resources (DERs) to relieve power flow stress in nowadays stressed power distribution networks. A microgrid, either producing or consuming electricity, typically connects to a power distribution network through a single point of common coupling (PCC). From the perspective of a distribution network operator, this PCC can be either a generator bus, a load bus, or even disconnected if the microgrid operates in stand-alone mode. As a load bus, unlimited power consumption from a microgrid will cause voltage collapse problem.

Power network enters a state of voltage collapse when system condition change causes an uncontrollable voltage drop [2]. Voltage collapse is mainly caused by power system's inability to supply enough reactive power, such as in a stressed power network. There is a growing concern about stressed power networks due to increasing electricity demand and aging infrastructure. Furthermore, power distribution networks operate closer to their voltage stability limits as DERs complicate network power flow. Since power distribution networks are vulnerable to voltage collapse, impending voltage instability needs to be detected accurately.

Compared with a stability condition derived using Lyapunov-based method [3], an indicator is preferred that shows a power system's closeness to voltage collapse. To detect potential voltage instability, continuation power flow was an option [4]. This continuation power flow method was used as a standard method and relied on an approximated power flow relationship [5]. Due to approximation, continuation power flow method is typically inaccurate unless a system collapse is about to happen. As pointed out in [4], complete knowledge of the entire power distribution network is required but usually unavailable. In addition, the continuation power flow method requires a complete power flow analysis whenever a change happens. Because a power network constantly changes with control and protection actions, continuation power flow method is not suitable for a microgrid.

Alternatively, loadability condition provides a critical load impedance at each load bus using either model-based or measurement-based method. In model-based method, a *Thevenin* equivalent circuit, reflecting relative strength, was obtained based on local measurements at each load bus [6][7]. Nevertheless, because accurate parameter estimation takes time, model-based method does not qualify for real-time applications. Moreover, this model-based method could not predict voltage stability even when future load forecast is available. To obtain a real-time voltage stability index, measurement-based method was proposed that required phase-angle information from phasor measurement units (PMUs) [8][9][10]. Along this direction, a wide-area voltage stability monitoring system [9][11] was developed that measured synchronized phase angles throughout a power network. These measurements lead to complete knowledge of the entire power network [12][13] to decide voltage stability margin. Load buses in a power distribution network, however, do not install PMUs. Neither approach analyzed static voltage stability for a microgrid without requiring excessive information.

To solve problems in existing voltage stability detection methods, a local voltage stability detector is pro-

[1]Z. Wang is with Department of Electrical Engineering, University of Notre Dame, Notre Dame, IN 46556, USA zwang6@nd.edu

[2]H. Sun and D. Nikovski are with Mitsubishi Electric Research Laboratories (MERL), Cambridge, MA 02139, USA hongbosun@merl.com, nikovski@merl.com

*This work was performed during Zhao Wang's internship at MERL.

posed for microgrids in a power distribution network. Different from continuation power flow method, this voltage stability detector uses power flow equations without approximation. The local detector determines an accurate voltage stability index for a microgrid, once local measurement is available at the microgrid's PCC. Unlike PMU-based monitoring systems in [9][10][11], only local states are examined to compute voltage stability index. Compared with model-based loadability conditions, this voltage stability detector has no time delay. In addition, the local detector even predicts voltage stability index once a local load forecast is available to a microgrid manager. The proposed detector, therefore, outperforms existing techniques.

The remainder of this paper is organized as follows. Section II introduces notations in this paper. Section III describes a power network model with key assumptions. Section IV introduces a static voltage stability index based on only local measurements. Section V demonstrates simulation results showing accurate detection of impending voltage collapse. Section VI provides conclusions of this voltage stability detector.

II. Notations

Three-phase balanced operation and per-unit (p.u.) normalization are basic assumptions. Under these assumptions, admittance matrix $\boldsymbol{Y}_{n\times n}$ of an n-bus power network is a complex matrix [14]. Shunt admittance at bus i is not included in $\boldsymbol{Y}_{n\times n}$, but considered as a shunt device in load model. Admittance matrix $\boldsymbol{Y}_{n\times n}$ is expressed as $\boldsymbol{Y}_{n\times n}=\boldsymbol{G}_{n\times n}+j\boldsymbol{B}_{n\times n}$, where $\boldsymbol{G}_{n\times n}$ is conductance matrix and $\boldsymbol{B}_{n\times n}$ is susceptance matrix. Each component of admittance matrix, i.e. Y_{ij}, is expressed in a rectangular form as $Y_{ij}=G_{ij}+jB_{ij}$ or in a polar form as $Y_{ij}=|Y_{ij}|\angle\phi_{ij}$ where $|Y_{ij}|=\sqrt{G_{ij}^2+B_{ij}^2}$ and $\phi_{ij}=\tan^{-1}(\frac{B_{ij}}{G_{ij}})$.

Each bus is assumed to connect a generator and a load. $P_{gen,i}$ and $Q_{gen,i}$ denote generated power; $P_{load,i}$ and $Q_{load,i}$ are real and reactive loads. At any bus i, E_i is voltage magnitude and δ_i is phase angle; P_i and Q_i are injected power; $\theta_{ij}=\delta_i-\delta_j$ is phase angle difference between any bus i and j. Power injections at bus i are

$$P_i=P_{gen,i}-P_{load,i} \text{ and } Q_i=Q_{gen,i}-Q_{load,i}.$$

With no power generation whatsoever, a pure load bus j has $P_j+P_{load,j}=0$ and $Q_j+Q_{load,j}=0$.

Using these state definitions, power injections P_i and Q_i at any bus i are expressed in *power flow* relationship

$$P_i=\sum_{j=1,j\neq i}^{n}|Y_{ij}|[E_iE_j\cos(\theta_{ij}-\phi_{ij})-E_i^2\cos\phi_{ij}], \quad (1)$$

$$Q_i=\sum_{j=1,j\neq i}^{n}|Y_{ij}|[E_i^2\sin\phi_{ij}+E_iE_j\sin(\theta_{ij}-\phi_{ij})]. \quad (2)$$

Parameters G_{ij}, B_{ij}, $|Y_{ij}|$ and ϕ_{ij} are initially determined by power network planning then vary constantly due to protection and control actions. Although possible in a power transmission system, keeping updated knowledge of the entire power distribution network is not realistic. Any effective voltage stability detector, therefore, should only use available local information.

A power network, or simply a microgrid, includes various types of loads that are represented in a ZIP load model [15] combining constant-impedance (Z), constant-current (I) and constant-power (P) components. Real and reactive loads at any bus i are defined as functions of voltage magnitude E_i (in p.u.) as

$$P_{load,i}=E_i^2P_{Z-load,i}+E_iP_{I-load,i}+P_{P-load,i}, \quad (3)$$

$$Q_{load,i}=E_i^2Q_{Z-load,i}+E_iQ_{I-load,i}+Q_{P-load,i}, \quad (4)$$

where $P_{Z-load,i}$ and $Q_{Z-load,i}$ are nominal constant-impedance loads, including shunt devices; $P_{I-load,i}$ and $Q_{I-load,i}$ are nominal constant-current loads, denoting devices that are modeled as current sources; $P_{P-load,i}$ and $Q_{P-load,i}$ are nominal constant-power loads, generally as a result of power control mechanism. This ZIP model, therefore, represents a variety of loads and control devices.

III. System Model

An n-bus power distribution network is modeled with m microgrids and l pure load buses, so that there is $n=m+l$. *Assumption* 1 and 2 are important to the voltage stability detector. *Assumption* 1 ensures a simple and accurate power flow expression at microgrid's PCC. *Assumption* 2 relates voltage collapse directly to insufficient reactive power support from a microgrid.

Assumption 1: Microgrid at bus i connects to power distribution network through PCC to pure load bus j.

Under this assumption, power flow in equations (1) and (2) simplifies to

$$P_i=E_iE_j|Y_{ij}|\cos(\theta_{ij}-\phi_{ij})-E_i^2|Y_{ij}|\cos\phi_{ij},$$
$$Q_i=E_i^2|Y_{ij}|\sin\phi_{ij}+E_iE_j|Y_{ij}|\sin(\theta_{ij}-\phi_{ij}).$$

Because power flow expressions are simplified with only three state variables, an accurate voltage stability index can be determined without approximation.

Assumption 2: When voltage instability happens to a microgrid, the microgrid's reactive power generation has reached its capacity limit.

If the microgrid has surplus reactive power capacity, it is able to control PCC voltage to prevent voltage collapse. Once reaching either upper or lower reactive power capacity limit, the microgrid's PCC converts from a voltage-regulated P-V bus to a P-Q bus.

In Figure 1, a general branch model describes the connection link between bus i and j, which is either a transmission line or a transformer with tap changer and tap value T_{ij}. Specifically, tap value of a transmission line is $T_{ij}=1$. With a little abuse of notation, Y_{ij} is defined as $Y_{ij}=-\frac{1}{Z_{ij}}$, which is expressed in either a rectangular form $Y_{ij}=G_{ij}+jB_{ij}$ or a polar form$Y_{ij}=$

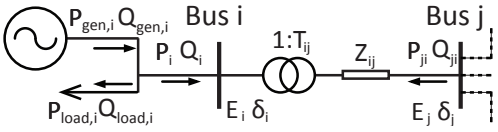

Fig. 1. General branch model for the connection link between bus i and bus j.

$|Y_{ij}|\angle\phi_{ij}$. The power flow expression in equations (1) and (2) transforms to

$$P_i = |Y_{ij}|\left[T_{ij}E_iE_j\cos(\theta_{ij}-\phi_{ij}) - T_{ij}^2E_i^2\cos\phi_{ij}\right], \quad (5)$$

$$Q_i = |Y_{ij}|\left[T_{ij}^2E_i^2\sin\phi_{ij} + T_{ij}E_iE_j\sin(\theta_{ij}-\phi_{ij})\right]. \quad (6)$$

Static voltage stability analysis focuses on the relationship between reactive power flow Q_i and voltage magnitude E_i. When a microgrid has surplus reactive power capacity, it usually controls voltage to a deviated value using a droop controller, leading to a regulated P-V bus. For instance, a traditional P-E droop controller can be used to manage voltage magnitude at a microgrid's PCC, with the following dynamics

$$\dot{E}_i = (E_{ref,i} - E_i) - m_{Q,i}Q_{gen,i},$$

where $m_{Q,i}$ is droop slope of the Q-E droop controller; $E_{ref,i}$ denotes voltage control command; $Q_{gen,i}$ is reactive power generation from the microgrid. With such a droop controller, the amount of injected power from a microgrid, i.e. $Q_{gen,i}$, is proportional to the voltage difference between $E_{ref,i}$ and E_i. The additional reactive power injection prevents voltage magnitude E_i from dropping further. When reactive power generation $Q_{gen,i}$ saturates at its capacity limit $Q_{max,i}$, there is no more voltage regulation from the microgrid, rendering a P-Q bus. As described in *Assumption* 2, voltage stability analysis studies a microgrid-connected bus that is a P-Q bus without voltage control.

To derive a static voltage stability index, reactive power flow expression is derived at the microgrid-connected bus i with its coupled load bus j as

$$\begin{aligned} Q_i &= Q_{max,i} - E_i^2Q_{Z-load,i} - E_iQ_{I-load,i} - Q_{P-load,i}, \\ &= T_{ij}^2E_i^2|Y_{ij}|\sin\phi_{ij} + T_{ij}E_iE_j|Y_{ij}|\sin(\theta_{ij}-\phi_{ij}). \end{aligned} \quad (7)$$

Combining coefficients of polynomials on both sides of the equation, the following equation is obtained

$$\begin{aligned} 0 &= a_iE_i^2 + b_iE_i + c_i, \quad (8) \\ \text{where } a_i &= Q_{Z-load,i} + T_{ij}^2|Y_{ij}|\sin\phi_{ij}, \\ b_i &= Q_{I-load,i} + T_{ij}E_j|Y_{ij}|\sin(\theta_{ij}-\phi_{ij}), \\ c_i &= Q_{P-load,i} - Q_{max,i}. \end{aligned}$$

Equation (8) provides a model to analyze static voltage stability at any microgrid-connected bus i.

IV. Main Result

Based on models in Section III, static voltage stability index is defined for microgrids in a power distribution network. Furthermore, method is proposed to predict voltage stability index once there is local load forecast.

As in equation (7), reactive power flow into bus i, i.e. Q_i, is expressed in two second-order polynomials of voltage magnitude E_i in (p.u.). These two polynomials correspond to two quadratic curves in the Q_i-E_i plane, as shown in Figure 2. Both light and heavy load situations are examined at a microgrid's PCC. Concave lines in Figure 2 are reactive power injection curves that represent equation (4); convex lines are reactive power flow curves that depict equation (6). For light-load situation, solid lines crosses at a voltage magnitude around 0.95 p.u. and reactive power injection value above zero, shown as the right triangle "Δ". When load increases in the microgrid, the power injection curve (in dashed line) shifts down while the power flow curve (in dashed line) raises up. As a result, operating point moves to the right circle "$\circ$" in Figure 2, which corresponds to a significant voltage drop by more than 0.4p.u.. As load level continues to increase, it is reasonable to predict that the operating point disappears, i.e. voltage collapse happens.

Based on graphic explanations in Figure 2, a static voltage stability index $\boldsymbol{I_{vs,i}}$ is introduced as follows.

Proposition 1: For a microgrid in a power distribution network that satisfies Assumption 1 and 2, a static voltage stability index $\boldsymbol{I_{vs,i}}$ at bus i is

$$\boldsymbol{I_{vs,i}} = \frac{\sqrt{b_i^2 - 4a_ic_i}}{a_i},$$

where $a_i = Q_{Z-load,i} + T_{ij}^2|Y_{ij}|\sin\phi_{ij}$, $b_i = Q_{I-load,i} + T_{ij}E_j|Y_{ij}|\sin(\theta_{ij}-\phi_{ij})$, and $c_i = Q_{P-load,i} - Q_{max,i}$. If the static voltage stability index is a real number with

$$\boldsymbol{I_{vs,i}} > 0,$$

then the microgrid has static voltage stability; if the real index $\boldsymbol{I_{vs,i}}$ is zero, voltage collapse happens.

Proof: For a microgrid in a power distribution network that satisfies Assumption 1 and 2, if the static voltage stability index is real and positive, there is

$$b_i^2 - 4a_ic_i > 0.$$

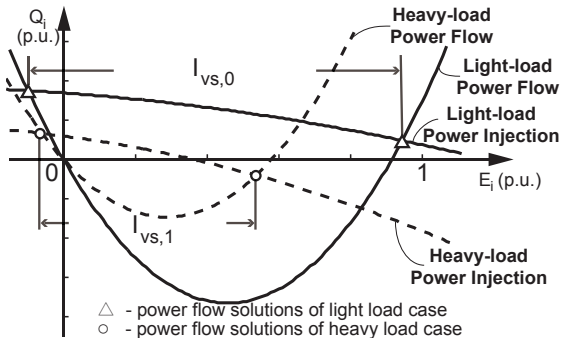

Fig. 2. Quadratic curves of $Q_i(E_i)$ at two load situations, with light load in solid line (operating point as the right triangle) and heavy load in dashed line (operating point as the right circle).

Equation (8) has two different real solutions

$$E_{u,i} = \frac{-b_i + \sqrt{b_i^2 - 4a_i c_i}}{2a_i} \text{ and } E_{l,i} = \frac{-b_i - \sqrt{b_i^2 - 4a_i c_i}}{2a_i}.$$

Among the two dissimilar real solutions, the larger solution $E_{u,i}$ corresponds to a feasible voltage magnitude yet the smaller one $E_{l,i}$ is unfeasible. As the real index $\boldsymbol{I_{vs,i}}$ decreases to zero, there is

$$b_i^2 - 4a_i c_i = 0,$$

and the two real solutions converge to a single one, i.e. $E_{u,i} = E_{l,i}$. Voltage collapse happens when power flow analysis provides no real solution, so that the critical situation corresponds to $\boldsymbol{I_{vs,i}} = 0$. ■

Remark 1: Static voltage stability index $\boldsymbol{I_{vs,i}}$, as a voltage magnitude difference, relates back to crossing points of the load power flow curve and the power injection curve in Figure 2.

Remark 2: Computation of index $\boldsymbol{I_{vs,i}}$ is purely algebraic so that is finished together with control algorithms at a microgrid's PCC. Once the index drops below a threshold, voltage control actions are triggered, such as connecting shunt devices or even shedding load.

Besides issuing a warning based on current measurement, it would be helpful for a microgrid manager to predict voltage stability in near future based on current voltage stability index. Since nonlinear power flow relationship cannot be approximated by a linear function of local load variations, a predictor based on Taylor series expansion usually underestimates voltage drop near the critical point. As a result, we propose to use the relationship between $\Delta Q_{load,i}$ and $\Delta \boldsymbol{I_{vs,i}}$ to predict voltage stability index with local load variation forecast at bus i as

$$\hat{\boldsymbol{I}}_{\boldsymbol{vs,i}}^{\boldsymbol{k+1}} = \boldsymbol{I}_{\boldsymbol{vs,i}}^{\boldsymbol{k}} + \Delta \hat{Q}_{load,i}(t_{k+1}) \frac{\Delta \boldsymbol{I}_{\boldsymbol{vs,i}}^{\boldsymbol{k}}}{\Delta Q_{load,i}(t_k)}. \quad (9)$$

where $\Delta \boldsymbol{I}_{\boldsymbol{vs,i}}^{\boldsymbol{k}}$ and $\Delta Q_{load,i}(t_k)$ are voltage stability index and reactive load variation over the time interval $t \in [t_{k-1}, t_k]$; $\Delta \hat{Q}_{load,i}(t_{k+1})$ is the predicted reactive load variation in the time interval $t \in [t_k, t_{k+1}]$. For a microgrid manager, $\boldsymbol{I}_{\boldsymbol{vs,i}}^{\boldsymbol{k}}$, $\Delta \boldsymbol{I}_{\boldsymbol{vs,i}}^{\boldsymbol{k}}$ and $\Delta Q_{load,i}(t_k)$ are accurately known at $t = t_k$, while $\Delta \hat{Q}_{load,i}(t_{k+1})$ is an estimated reactive load change. Because time interval is short for voltage stability prediction, these predictions are accurate. Using this index $\hat{\boldsymbol{I}}_{\boldsymbol{vs,i}}^{\boldsymbol{k+1}}$, a microgrid manager instantly determines whether local load variation causes the entire power distribution network dangerously close to voltage collapse.

V. Simulation Test

The static voltage stability detector is examined in an IEEE nine-bus simulation model, as shown in Figure 3. The simulation network model is obtained from [16] and modified to include three microgrids. Each microgrid connects to the power distribution network through a transformer with tap changer. Each step-up transformer has nine taps (between 0.95p.u. and 1.05p.u.) at its high-voltage side that automatically regulate voltage at the PCC of each microgrid. Each tap change corresponds to a 0.0125p.u. (or 1.25%) of voltage magnitude variation with a mechanical delay of 4.0 seconds. There is information exchange between both sides of each transformer so that voltage E_j and power flow from bus j to bus i are available at the microgrid's PCC at bus i. Besides these measurements, there is *NO* global communication in this power distribution network, which is typical in a power system.

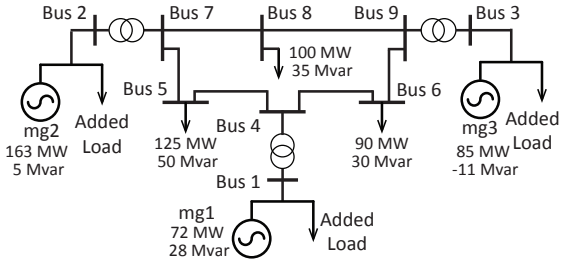

Fig. 3. Modified IEEE nine-bus network with microgrids.

Under this information exchange set-up, neither continuation power flow method nor critical loadability conditions can be applied these microgrids. For continuation power flow, it is impossible to determine a searching direction without complete knowledge of all states in a power system. Even if global measurements are available, power flow analysis is required every time the network parameter changes, such as tap change at any one of three transformers. Critical loadability conditions cannot be used in this realistic power network, either. Model-based approaches need time to estimate impedance accurately, but the power network may have changed over this time. Measurement-based methods require synchronized phasor measurements of the entire network, which is unavailable in a realistic power distribution network. Compared with these existing methods, the proposed voltage stability index is easily examined in real-time so that impending voltage collapse can be accurately detected.

The network in Figure 3 operates with a nominal frequency of 60Hz and a base power of 100MVA. Pure load buses are constant-power loads, whose values are shown in Figure 3. At each pure load bus, there is also a normally distributed noise with a standard deviation of 2.5% of nominal value. Increased load at a microgrid's PCC is a constant-power load that has a major component of reactive power with a power factor of 0.2. Voltage collapse, therefore, can be examined before the power network enters other forms of instability.

Each microgrid's PCC is controlled by a droop controller with generation capacity limits, whose parameters are shown in Table I. Frequency dynamics are simulated using swing equations with parameter M

and D. Different generation sources are installed in each microgrid so that parameters M_i and D_i are different. As shown in Table I, Bus 1 is based on a rotational generator, so that its inertia value M is large; bus 2 and bus 3 connect to microgrids with a fast-inverter based droop controller hence have small M values. Similarly, droop controller parameter $m_{Q,i}$ at each microgrid's PCC relates to the maximum reactive power support from each microgrid, i.e. $[\underline{Q}_{gen,i}, \overline{Q}_{gen,i}]$.

At the beginning of simulation, local load at each of three microgrids increases from zero to a peak value between $t = 5$sec and $t = 25$sec, stays for five seconds and recovers to the original value in a linear fashion between $t = 30$sec and $t = 50$sec. Over a period of twenty seconds, this local load variation is slow enough such that no transient exists.

Simulation results are demonstrated in the following figures, voltage in Figure 4, real power and reactive power in Figure 5. Reactive load level at bus 1 increases from zero to 3.25p.u., with a composition stated earlier. Reactive load increases at bus 2 and bus 3 are 25% of 3.25p.u., i.e. 0.8125p.u.. During the simulation, reactive power generation limit at bus 1 is reached while the other two microgrids still provide voltage regulation at bus 2 and bus 3. As shown in Figure 4, voltage magnitude at bus 1 drops from 1.04p.u. to around 0.65p.u.. Although voltage drop may trigger protection mechanisms, this power distribution network with microgrids has the capability to ride through low voltage. The impact of transformer tap change is obvious in plots of voltage, real power and reactive power. Such control and protection actions change the power distribution network constantly and make voltage stability analysis difficult. Even in this situation, performance of the voltage stability detector is satisfactory using only local information at each microgrid's PCC.

Performance of the voltage stability detector at all three microgrids is demonstrated in Figure 6. At bus 1, 2 and 3, the predicted value of voltage stability index $\hat{\boldsymbol{I}}_{\boldsymbol{vs},\boldsymbol{i}}$ in dashed line follows closely to the true value $\boldsymbol{I}_{\boldsymbol{vs},\boldsymbol{i}}$ in solid line. The error between the two curves is indistinguishable, whose maximum is below 0.05p.u.. This error, however, is not a problem for a tap-changing transformer with heavy load (such as bus 1) because the transformer is already saturated at its maximum tap. Tap positions of all three transformers are demonstrated in Figure 7, showing that the tap at bus 1 saturates at 1.05p.u. around $t = 26$sec. As load

TABLE I

DROOP CONTROLLER PARAMETER AT EACH MICROGRID'S PCC

#	m_Q p.u.	M $\frac{p.u.}{(\frac{rad}{s})^2}$	D $\frac{p.u.}{\frac{rad}{s}}$	ω_0 $\frac{rad}{s}$	$\underline{P}_{gen,i}$ $\overline{P}_{gen,i}$	$\underline{Q}_{gen,i}$ $\overline{Q}_{gen,i}$
1	0.05	0.0507	0.1959	120π	$[0.6, 1.37]$	$[-3.0, 3.0]$
2	0.033	0.0032	0.3138	120π	$[1.0, 2.0]$	$[-4.0, 4.0]$
3	0.05	0.0023	0.2315	120π	$[0.7, 1.4]$	$[-3.0, 3.0]$

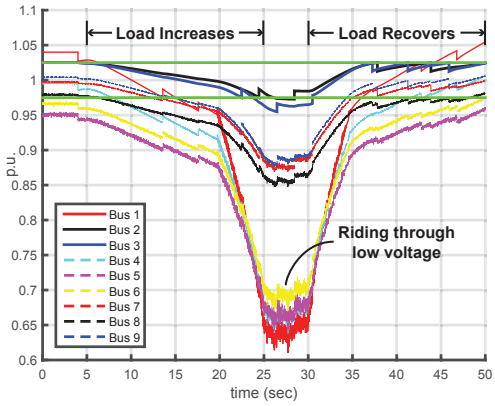

Fig. 4. Voltage on all buses of the IEEE nine-bus network: voltage jumps when tap changes at each microgrid-connected transformer; voltage at bus 1 drops from 1.04p.u. to around 0.55p.u..

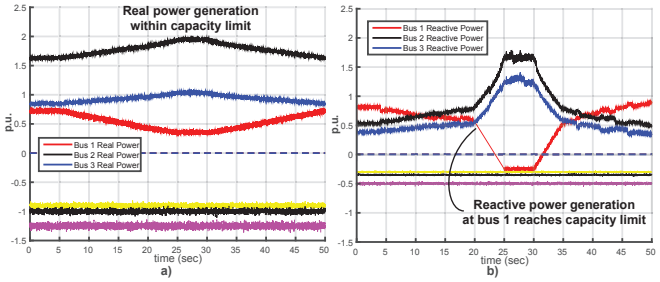

Fig. 5. Real and reactive power injection at all buses of the IEEE nine-bus network: a) real power generations are within capacity limits of all three microgrids; b) reactive power injection from microgrids at bus 2 and 3 maintains voltage regulation.

increases in the microgrid at bus 1, the voltage stability index at bus 1 decreases to around 0.6p.u.. Because the voltage stability index $\boldsymbol{I}_{\boldsymbol{vs},\boldsymbol{1}}$ still has margin, the power distribution network still maintains voltage stability and is able to ride through low voltage. A local voltage stability index is computed at each of the other two microgrids, as illustrated in blue and red in Figure 6. The voltage stability index at either bus 2 or bus 3 maintains above 1.0p.u., indicating voltage stability at these buses.

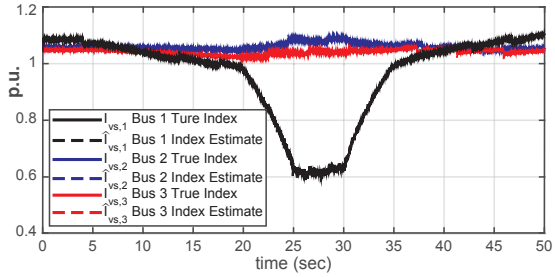

Fig. 6. Voltage stability index $\boldsymbol{I}_{\boldsymbol{vs},\boldsymbol{1}}$ at bus 1 (black); $\boldsymbol{I}_{\boldsymbol{vs},\boldsymbol{2}}$ at bus 2 (blue); $\boldsymbol{I}_{\boldsymbol{vs},\boldsymbol{3}}$ at bus 3 (red).

The static voltage stability detector is examined in this IEEE nine-bus simulation model showing how

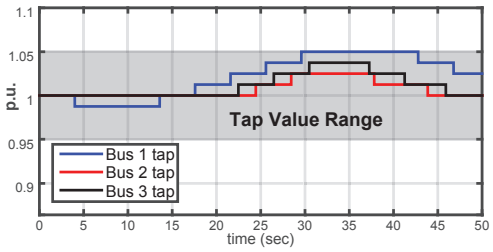

Fig. 7. Tap positions of all three step-up transformers.

impending voltage instability situations are predicted. The operation scenario is very realistic for a microgrid in a power distribution network, where the static voltage stability index is examined and predicted conveniently. However, under the same condition, continuation power flow method and critical loadability conditions cannot be applied. As a result, the voltage stability detector outperforms existing methods.

VI. Conclusion

To predict impending voltage collapse for microgrids in a power distribution network, this paper introduces a static voltage stability detector that only uses local measurements available at microgrid's PCC. The local stability detector derives a voltage stability index that indicates the distance of microgrid's power consumption from causing voltage collapse. The smaller the index, the more urgent a control action is required from the microgrid. Voltage stability detector updates the index whenever a local measurement is available. A prediction of voltage stability index is also made once the microgrid has a local load forecast. Compared with existing techniques, this voltage stability detector is accurate and easy to implement for a microgrid-integrated power distribution network.

In future work, the proposed detector will be compared with existing methods using large-scale power networks. Furthermore, a global management system will be laid on top of the distributed detector at each microgrid's PCC. Instead of phasor measurements, this global manager uses high-level voltage instability index $\hat{\boldsymbol{I}}_{\boldsymbol{vs,i}}$ to coordinate various microgrids in a power distribution network. An optimal operation scenario can then be achieved that improves voltage stability and reduces load shedding cost.

APPENDIX

Parameter of the connection link between a microgrid at bus i and pure load bus j is determined to compute voltage stability index. For a transmission line, parameters are $|Y_{ij}|$ and ϕ_{ij}; if a transformer with tap changer is used, parameters include $|Y_{ij}|$, ϕ_{ij} and T_{ij}. Available measurements include: real and reactive power injections at bus i, i.e. P_i and Q_i; real and reactive power flow from bus j to bus i, i.e. P_{ji} and Q_{ji}; voltage magnitudes at bus i and j, i.e. E_i and E_j.

For a transmission line, its parameters $|Y_{ij}|$ and ϕ_{ij} are determined as

$$\phi_{ij} = \tan^{-1}\left(\frac{Q_{ji}+Q_i}{-P_{ji}-P_i}\right) \text{ and } |Y_{ij}| = \frac{P_i^2+Q_i^2}{E_i^2(b_{L,i}+c_{L,i})},$$

where $b_{L,i} = Q_{ji}\sin\phi_{ij} - P_{ji}\cos\phi_{ij}$ and $c_{L,i} = Q_i\sin\phi_{ij} - P_i\cos\phi_{ij}$.

For a transformer with tap changer that automatically regulates voltage magnitude, parameters ϕ_{ij}, $|Y_{ij}|$, and T_{ij} are determined as

$$\phi_{ij} = \tan^{-1}\left(\frac{Q_{ji}+Q_i}{-P_{ji}-P_i}\right), \theta_{ij} = \tan^{-1}\left(\frac{a_{T,i}}{\frac{P_i^2+Q_i^2}{b_{T,i}+c_{T,i}} - c_{T,i}}\right),$$

$$|Y_{ij}| = \frac{c_{T,i} + \frac{a_{T,i}}{\tan(\delta_i-\delta_j)}}{E_i^2}, \text{ and } T_{ij} = \frac{a_{T,i}}{|Y_{ij}|E_iE_j\sin(\delta_i-\delta_j)},$$

where $a_{T,i} = P_i\sin\phi_{ij} + Q_i\cos\phi_{ij} = -P_{ji}\sin\phi_{ij} - Q_{ji}\cos\phi_{ij}$, $b_{T,i} = Q_{ji}\sin\phi_{ij} - P_{ji}\cos\phi_{ij}$ and $c_{T,i} = Q_i\sin\phi_{ij} - P_i\cos\phi_{ij}$.

References

[1] R. Lasseter, "Smart distribution: Coupled microgrids," *Proceedings of the IEEE*, vol. 99, no. 6, pp. 1074–1082, 2011.

[2] P. Kundur, *Power system stability and control*. Tata McGraw-Hill Education, 1994.

[3] P.-A. Lof, G. Andersson, and D. Hill, "Voltage stability indices for stressed power systems," *Power Systems, IEEE Transactions on*, vol. 8, no. 1, pp. 326–335, 1993.

[4] V. Ajjarapu, *Computational techniques for voltage stability assessment and control*. Springer Science & Business Media, 2007.

[5] V. Ajjarapu and C. Christy, "The continuation power flow: a tool for steady state voltage stability analysis," *Power Systems, IEEE Transactions on*, vol. 7, no. 1, pp. 416–423, 1992.

[6] K. Vu, M. M. Begovic, D. Novosel, and M. M. Saha, "Use of local measurements to estimate voltage-stability margin," *Power Systems, IEEE Transactions on*, vol. 14, no. 3, pp. 1029–1035, 1999.

[7] A. Wiszniewski, "New criteria of voltage stability margin for the purpose of load shedding," *Power Delivery, IEEE Transactions on*, vol. 22, no. 3, pp. 1367–1371, 2007.

[8] B. Milosevic and M. Begovic, "Voltage-stability protection and control using a wide-area network of phasor measurements," *Power Systems, IEEE Transactions on*, vol. 18, no. 1, pp. 121–127, 2003.

[9] M. Zima, M. Larsson, P. Korba, C. Rehtanz, and G. Andersson, "Design aspects for wide-area monitoring and control systems," *Proceedings of the IEEE*, vol. 93, no. 5, pp. 980–996, 2005.

[10] R. Sodhi, S. Srivastava, and S. Singh, "A simple scheme for wide area detection of impending voltage instability," *Smart Grid, IEEE Transactions on*, vol. 3, no. 2, pp. 818–827, 2012.

[11] J.-H. Liu and C.-C. Chu, "Wide-area measurement-based voltage stability indicators by modified coupled single-port models," *Power Systems, IEEE Transactions on*, vol. 29, no. 2, pp. 756–764, 2014.

[12] A. Phadke, J. Thorp, and K. Karimi, "State estimlation with phasor measurements," *Power Systems, IEEE Transactions on*, vol. 1, no. 1, pp. 233–238, 1986.

[13] C. W. Taylor, D. C. Erickson, K. E. Martin, R. E. Wilson, and V. Venkatasubramanian, "Wacs-wide-area stability and voltage control system: R&d and online demonstration," *Proceedings of the IEEE*, vol. 93, no. 5, pp. 892–906, 2005.

[14] A. R. Bergen, *Power Systems Analysis, 2/E*. Pearson Education, 2009.

[15] "Load representation for dynamic performance analysis," *Power Systems, IEEE Transactions on*, vol. 8, no. 2, pp. 472–482, 1993.

[16] A.-H. Amer, "Voltage collapse prediction for interconnected power systems," Ph.D. dissertation, West Virginia University, 2000.